MODELING GRAVITY-DRIVEN RIVULET ON A MONOTONICALLY VARYING INCLINE

M. Isoz [1]

[1] **Department of Mathematics, Faculty of Chemical Engineering, University of Chemistry and Technology, Studentska 5, 166 28 Prague, Czech Republic**

Abstract

Rivulet type flow is of great importance in many engineering areas including the packed columns design or heat exchangers calculations. We concentrate on the case of a rivulet flowing in the azimuthal direction from top to bottom of a large horizontal cylinder. A direct numerical simulation of the problem is compared to simplified solutions of the Navier-Stokes equations for the cases of a rivulet with (i) constant contact angle and varying width, (ii) constant width and varying contact angle, and (iii) varying both contact angle and width. Such comparison sheds light on the applicability of simplified models for a solution of real-life problems.

Keywords: rivulet, fluid dynamics, liquid spreading.

1 Introduction

Flow characteristics of a gravity-driven spreading trickle of a liquid is of key importance throughout many areas of chemical engineering, including the mass transfer [1], trickle bed reactors [2], heat exchangers [3] and various coating processes [4].

Eventhough the rivulet type flow can be modeled using various CFD methods [1,5], such methods are still too complex to be used in the engineering practice and too computationally demanding for the parametric studies of the rivulet behavior.

A simplified solution to the problem of the rivulet type flow has been studied since 1960's. The pioneering studies by Towell and Rothfeld [6], Allen and Biggin [7], Bentwich et al. [8] and Fedotkin et al. [9] have led to a substantial amount of subsequent work on a rectilinear rivulet flow. For example, Benilov [10] performed a stability analysis for the rivulet flow down an inclined substrate and Duffy and Moffat [11] used the solution available for the rectilinear rivulet flow to describe the flow with prescribed volume flux and non-zero contact angle over a cylinder of large radius. For further informations on the topic of unidirectional (rectilinear) rivulet flow, see [12] and many references therein.

The physics of the contact line region of a rivulet was first taken into account by Davis [13] and revisited from another point of view by Shetty and Cerro [14]. However, a literature covering the topic of modeling the flow of a spreading rivulet is still limited to various CFD methods (e.g. [1,15,16]) or the spreading rivulet stability analysis (see [17] and references therein).

In our previous work, we derived a computationally inexpensive method to determine the size of the gas-liquid interface of a rivulet flowing down an inclined wetted plate (see [18] and references therein). We have also focused on possibilities of modeling such a flow in OpenFOAM, the most widely used opensource CFD software [19].

In the present work, we generalize the developed method for the case of the flow in the azimuthal direction from top to bottom of a large horizontal cylinder. We compare the obtained results with CFD experiment carried out in the OpenFOAM software as well as with results obtained from other simplified analytical solutions to the studied problem [11,12].

Such a comparison permits to evaluate a legitimacy of assumptions made during the method derivation. Furthermore, the presented results offer, within accuracy limitations of the used CFD methods, a baseline for usability assessment of the simplified models.

2 Coordinate system and simplifying assumptions

To be able to derive the different analytical solutions, the system of the Navier-Stokes equations was simplified under the following assumptions:

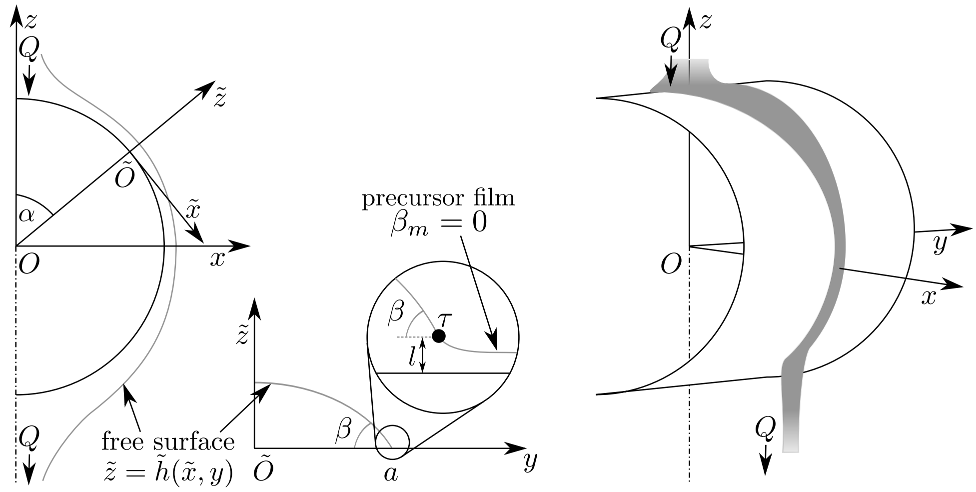

Figure 1: A particular coordinate system with basics of the used rivulet spreading notation. The global coordinate system is denoted by (O, x, y, z). At each surface inclination angle, α, a local coordinate system denoted by $(\tilde{O}, \tilde{x}, \tilde{y}, \tilde{z})$ is introduced to obtain the simplified solutions. The dynamic and microscopic contact angles [20] are denoted as β and β_m, respectively. The letter a stands for the rivulet half width. The point where the outer and inner solutions for $\tilde{h}(\tilde{x}, \tilde{y})$ (rivulet profile with respect to local coordinate system) are stitched together is denoted by τ. We also introduce the cylinder radius, R, and arc length coordinate, $s = \alpha R$.

1. The studied liquid is Newtonian with constant density, ρ, dynamic viscosity, μ, and surface tension, γ.
2. The rivulet profile shape is constant in time. Furthermore, rivulet liquid flow rate is assumed to be constant along the cylinder.
3. There is no shear between the gas and liquid phases.
4. The liquid velocities in the directions transversal and normal to the cylinder are negligible in comparison to the one in its longitudinal direction, $\tilde{u} \gg \tilde{v} \sim \tilde{w}$. The inertial effects can be neglected in $\tilde{y}$ and $\tilde{z}$ directions.
5. The gravity is the only acting body force.
6. The gravity effects on the velocity of the contact lines are neglected. Also the dynamic contact angles, $\beta = \beta(s)$, are assumed small all along the rivulet.
7. There is a thin precursor film on the whole studied surface. Thus, the microscopic contact angle $\beta_m = 0$. Furthermore, no contact angle hysteresis is taken into account.
8. The intermediate region length scale well separating the inner and outer solution for the profile shape [20] corresponds to the height scale of the precursor film, l.

In the case of CFD, only the assumption of a shallow rivulet, $\beta \ll 1$, was retained and the solution was obtained using the lubrication approximation.

3 Simulation methods

Altogether, we examined four different methods to simulate a rivulet flowing down a slowly varying incline. All calculations are based on the thin film governing equation,

$$h_t - \frac{1}{3\mu} \nabla \cdot \left[\left(h^3 + 3\lambda h^2 \right) \left(\rho g \nabla h - \gamma \nabla \kappa \right) \right] = 0, \tag{1}$$

where λ stands for the Navier slip length and κ for the gas-liquid interface mean curvature.

As a benchmark model, a CFD simulation carried out in OpenFOAM software was used. Within this simulation, the equation (1) was solved directly, using the finite volume method. The remaining three methods were all derived by solving a simplified version of the equation (1) analytically.

In the following text, we will at first briefly introduce the thin film governing equation itself. Then we will present its simplifications for the studied case of a rivulet flow down an azimuthal direction of a large cylinder.

Thin film governing equation

The thin film governing equation, (1), can be derived from the Navier-Stokes equations using the so called lubrication approximation. This approximation is based on the assumption of a thin film flow, which permits to average all the variables in one of the spatial directions.

With the above mentioned averaging, it is possible to partially integrate the Navier-Stokes equations and to express all the original variables (velocity and pressure fields) via a function, denoted h, defining the shape of the gas-liquid interface (or, the problem free boundary position) [21].

Let us now examine in more detail the equation (1) itself, more precisely its second term, which is problem dependent. In the presented case, we assumed a shallow rivulet with the gas-liquid interface shaped by the gravity and surface tension. Hence, the second factor of the studied equation term has the form of $\rho g \nabla h - \gamma \nabla \kappa$.

Moreover, one can take the first factor in the studied equation term, $h^3 + 3\lambda h^2$, as a place of the application of the forces expressed in the second factor. Within this analogy, h^3 represents the liquid volume. The presence of the term $3\lambda h^2$ is a direct consequence of the need to address the formal divergence of the energetic functional at the rivulet three phase lines caused by the application of the no-slip boundary condition at the substrate [22].

One of the ways to formally provide an upper bound for the energy necessary to move a contact line is to replace the no-slip boundary condition at the substrate by a less restrictive one in the form of

$$\tilde{z} = 0, \quad \vec{n} \cdot u = 0, \quad u - \vec{t} \cdot \lambda \nabla u = 0\,, \tag{2}$$

where $\vec{n}$ is the outer unit normal to the boundary and $\vec{t}$ is the unit tangent to the boundary. The boundary condition (2) allows a small ($\lambda \ll 1$) slip at the substrate, thus the energy needed to move the liquid onto an unwetted area is finite.

Finally, the equation (1) needs to be completed by a set of boundary conditions. Using the notation specified in Fig. 1, the proposed boundary conditions are,

$$\begin{aligned} \tilde{y} = \pm a, \qquad \qquad \tilde{h} &= 0 \\ \vec{n}_\tau \cdot \nabla \tilde{h} &= \pm \tan \beta \\ \nabla \cdot (\nabla \nabla \tilde{h}) &= \dot{\tau} \end{aligned} \tag{3}$$

where $\vec{n}_\tau$ is the outer unit normal to the rivulet contact line in τ and $\dot{\tau}$ is the local speed of τ movement describing the dynamics of the rivulet spreading.

For the case of the benchmark CFD model, we continued the simulation that consists of solving the non-stationary equation (1) subject to boundary conditions (3) until

$$\tilde{y} = \pm a, \quad \nabla \cdot (\nabla \nabla \tilde{h}) = 0, \tag{4}$$

which corresponds to a pseudo-steady state of the system.

Simplifying the thin film governing equation

Under the assumptions listed in the section 2, the equation (1) can be further simplified. At first, we will present the solution for a rivulet with a constant width and contact angle (a static rivulet) as it was published by Duffy and Moffat [11]. Then we will leverage this solution to obtain models for the rivulet type flow down a slowly varying incline for the cases of a rivulet with fixed either contact angle or width derived by Paterson et al. [12]. Finally, we will combine the solution for a static rivulet with the Cox-Voinov law [20,23,24] to obtain a model for the case of the rivulet with varying both the contact angle and width.

Let us assume a gravity driven rivulet with no variations in the gas-liquid interface shape along its main flow direction, $\tilde{x}$, flowing down a plate inclined by an angle α to the horizontal. The equation (1) and boundary conditions (3) can be simplified to

$$\begin{aligned} &\tilde{y} \in (-a, a), \quad \gamma \tilde{h}_{\tilde{y}\tilde{y}\tilde{y}} - \mathrm{B}^2 \tilde{h}_{\tilde{y}} &&= 0 \\ &\tilde{y} = \pm a, \qquad\qquad\qquad\qquad \tilde{h} &&= 0 \\ &\qquad\qquad\qquad\qquad\qquad\quad\; \tilde{h}_{\tilde{y}} &&= \pm \tan\beta, \end{aligned} \tag{5}$$

where B is the Bond number of the problem, $\mathrm{B} = a\sqrt{\rho g |\cos\alpha|/\gamma}$, that represents the ratio of volume and surface forces in the rivulet. By $\tilde{h}_y$ we denote a derivative of $\tilde{h}$ with respect to $\tilde{y}$ as for the case of the profile shape constant along the $\tilde{x}$ coordinate $\tilde{h} = \tilde{h}(\tilde{y})$.

The problem (5) may be integrated analytically and the resulting profile shape function, $\tilde{h}$, for three cases of a different substrate inclination angle, $\alpha < \pi/2$, $\alpha = \pi/2$ and $\alpha > \pi/2$ denoted as (i), (ii) and (iii) is,

$$\tilde{h}(\zeta) = \begin{cases} \dfrac{a\tan\beta}{\mathrm{B}} \left(\dfrac{\cosh \mathrm{B} - \cosh \mathrm{B}\zeta}{\sinh \mathrm{B}} \right) & (i) \\ \dfrac{a\tan\beta}{2} (1 - \zeta^2) & (ii) \\ \dfrac{a\tan\beta}{\mathrm{B}} \left(\dfrac{\cos \mathrm{B}\zeta - \cos \mathrm{B}}{\sin \mathrm{B}} \right) & (iii) \end{cases}, \tag{6}$$

with ζ being the $\tilde{y}$ coordinate scaled by the rivulet half-width, $\zeta = \tilde{y}/a$.

The cases (i) and (iii) of the solution (6) have a singularity at $\mathrm{B} = 0$. Furthermore, the case (iii) has a singularity at $\mathrm{B} = \pi$ and thus is only sensible if B is restricted by $0 < \mathrm{B} < \pi$. To encounter the singularity at $\mathrm{B} = 0$, one would have to assume a rivulet of a zero width or a liquid with either zero density, or infinite surface tension, which is unphysical. On the other hand, the singularity of the case (iii) at $\mathrm{B} = \pi$ corresponds to the dripping of the liquid from the substrate. The dripping occurs at high B, when the surface tension forces are not strong enough to counteract the effects of the gravity and keep the rivulet in contact with the surface.

With the liquid volumetric flux taken as a fixed parameter, the rivulet half width, a, and its apparent contact angle, β, are bound together by the equation,

$$\frac{Q}{a} = \int_{-1}^{1} \int_{0}^{\tilde{h}(\zeta)} u(\zeta, \tilde{z})\, \mathrm{d}\tilde{z}\, \mathrm{d}\zeta = \int_{-1}^{1} \int_{0}^{\tilde{h}(\zeta)} \frac{\rho g \sin\alpha}{2\mu} \left(2\tilde{h}(\zeta)\tilde{z} - \tilde{z}^2 \right) \mathrm{d}\tilde{z}\, \mathrm{d}\zeta\, . \tag{7}$$

Evaluating the integral in (7), one obtains the following relation for the rivulet contact angle and half width,

$$\frac{\mu Q}{a^4 \rho g \sin\alpha \tan^3\beta} = F(\mathrm{B})\, . \tag{8}$$

The right hand side of the equation (8) has the form

$$F(\mathrm{B}) = \begin{cases} \dfrac{54\mathrm{B}\cosh \mathrm{B} + 6\mathrm{B}\cosh 3\mathrm{B} - 27\sinh \mathrm{B} - 11\sinh 3\mathrm{B}}{36\mathrm{B}^2 \sinh^3 \mathrm{B}} & (i) \\ \dfrac{4}{105} & (ii) \\ \dfrac{27\sin \mathrm{B} + 11\sin 3\mathrm{B} - 54\mathrm{B}\cos \mathrm{B} - 6\mathrm{B}\cos 3\mathrm{B}}{36\mathrm{B}^2 \sin^3 \mathrm{B}} & (iii) \end{cases} \tag{9}$$

In the studied case of a rivulet flowing down the azimuthal direction of a large cylinder, the substrate inclination angle, α, is a function of the arc length coordinate, s. Consequently, also the shape of the gas-liquid interface will change with s.

The equation (8) is the base stone of all three analytic methods. Furthermore, it inherits the singularities at $\mathrm{B} = 0$ and $\mathrm{B} = \pi$ of the equation (6). Hence, we propose a brief reflection on its behavior in dependence on the substrate inclination angle and the problem Bond number before we proceed with the derivation of the methods.

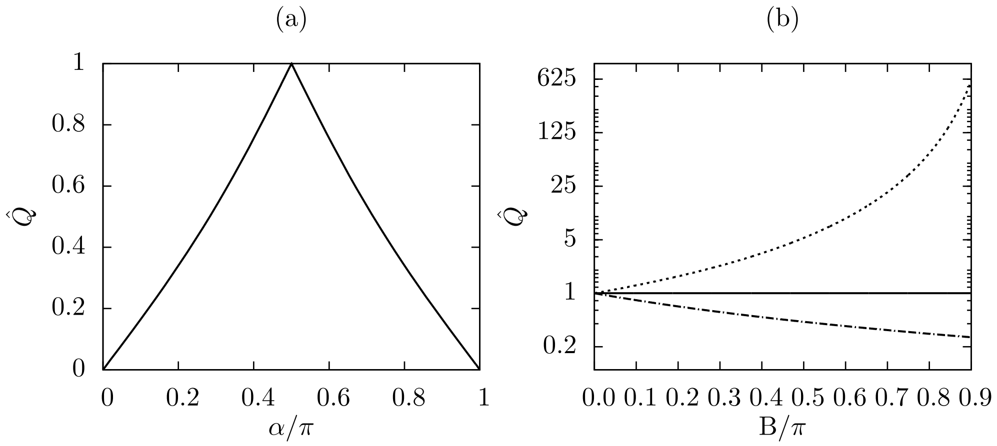

Figure 2: Dependence of the dimensionless flow rate, $\hat{Q}$, on the plate inclination angle, (a), and on the Bond number, (b). In the Figure on the right side are distinguished the three different cases, (i) for $\alpha < \pi/2$ (▪·▪··), (ii) for $\alpha = \pi/2$ (▬) and (iii) for $\alpha > \pi/2$ (▪▪▪).

In Fig. 2, there is depicted the dependence of the liquid flow rate on the substrate inclination angle and on the problem Bond number. The liquid volumetric flow rate, Q, is scaled by the flow rate in the rivulet on a vertical substrate,

$$\hat{Q} = \frac{105\mu}{4a^4\rho g \sin\alpha \tan^3\beta} Q = \frac{105\rho g\mu \cos^2\alpha}{4\gamma^2 \sin\alpha \tan^3\beta} \frac{Q}{\mathrm{B}^4} \,. \tag{10}$$

Please note, that we assumed a physically correct scenario of a rivulet with $a > 0$ and a liquid with $\rho > 0$ and $0 < \gamma < K \in \mathbb{R}^+$. Hence, the following asymptotic behavior of the dimensionless liquid flow rate for the three different cases of the substrate inclination angle can be observed,

$$\begin{aligned} (i) - (iii): &\quad \lim_{\mathrm{B}\to 0_+} \hat{Q}(\mathrm{B}) = 1 \\ (i): &\quad \lim_{\mathrm{B}\to \infty} \hat{Q}(\mathrm{B}) = 0 \\ (iii): &\quad \lim_{\mathrm{B}\to \pi_-} \hat{Q}(\mathrm{B}) = \infty \end{aligned} \tag{11}$$

The proposed generalization of the model of a static rivulet flowing down an inclined plane for the studied geometry is based on an approximation of the evolving rivulet by a consecutive series of static ones. Then, in the cases of a rivulet with fixed width or contact angle, it is possible to obtain the shape of the rivulet gas-liquid interface on the cylinder via the following algorithm,

Algorithm 1 *Interface reconstruction method for the case of a fixed rivulet width*

1. *Fix the rivulet half width, a, keep the contact angle variable, $\beta = \beta(s)$.*
2. *Discretize the domain $\Omega = \{s \in (0,\pi)\}$ to N subdomains.*
3. *For i from 1 to N do:*
   (a) *substitute the current s_i into the equation* (8) *and obtain the missing gas-liquid interface defining parameter, a_i*
   (b) *get the current profile, $\tilde{h}_i(\tilde{y})$, from the equation* (6)
4. *Reconstruct the approximate gas-liquid interface position using the assumption*

$$\tilde{h}(s,\tilde{y}) \doteq \tilde{h}(s_i,\tilde{y}), \quad \forall s \in (s_i - \frac{1}{2}\delta_i, s_i + \frac{1}{2}\delta_i); \quad i = 1,2,\ldots,N$$

Remark 1 *The interface reconstruction algorithm for the case of a fixed rivulet contact angle is analogical to the Algorithm 1. The only difference is a mutual swapping of the variables a and β.*

In the case of a rivulet with both contact angle and width varying, these two quantities have to be linked together. We suggest a link based on the Cox-Voinov law [23,24],

$$\beta(t)^3 = 9\frac{\mathrm{d}a(t)}{\mathrm{d}t}\frac{\mu}{\gamma}\ln\left(\frac{a(t)}{2e^2 l}\right), \tag{12}$$

where $a(t)$ is the object characteristic dimension. The Cox-Voinov law is again a result of a partial integration of a simplified version of the thin film governing equation (1). This time we consider the case of a narrow, axially symmetric stripe of a liquid spreading on a horizontal substrate. Furthermore, in such the case $a(t)$ represents the stripe half width.

The Cox-Voinov law is a first order ordinary differential equation for two unknown functions, $\beta(t)$ and $a(t)$ and one free parameter, l, corresponding to the intermediate region length scale (see Fig. 1 and [20,23,24]).

In the case of a steady rivulet of a liquid flowing and spreading down the azimuthal direction of a large cylinder, the time coordinate in (12) has to be transformed to the spatial coordinate, s.

The proposed transformation from time to the spatial coordinate arises from the last assumption in the section Coordinate system and simplifying assumptions, (see page 1). We assume presence of a precursor film of a thickness corresponding to the intermediate region length scale, l, on the whole substrate. Thus the profile shape has an inflection point denoted τ and fixed in a constant height, l, above the cylinder hull.

Neglecting the long-range intermolecular forces, this precursor film can be taken as a free falling film. Hence, τ is moving along the s coordinate with the speed of

$$u_\tau = \frac{\rho g \sin\alpha(s)}{2\mu} l^2 \,. \tag{13}$$

The estimate for the speed of τ (13) can be used to obtain the needed transformation,

$$t = \frac{2\mu}{\rho g l^2 \sin\alpha} s, \quad \mathrm{d}t = \frac{2\mu(R\sin\alpha - s\cos\alpha)}{\rho g l^2 R \sin^2\alpha}\mathrm{d}s, \quad \alpha = \frac{s}{R}\,, \tag{14}$$

where R is the cylinder radius.

After the substitution from (14) into (12), one arrives at the following relation,

$$\frac{\mathrm{d}a}{\mathrm{d}s} = \frac{2\gamma(R\sin\alpha - s\cos\alpha)\beta^3}{9\rho g l^2 R \sin^2\alpha \ln[a/(2\mathrm{e}^2 l)]}\,, \tag{15}$$

providing the needed link between the width of the rivulet and its apparent contact angle. Then, based on the equations (8) and (15), we propose an algorithm for a gas-liquid interface reconstruction of a rivulet with variable both width and contact angle,

Algorithm 2 *Interface reconstruction method for the case of a variable rivulet width and contact angle*

1. *Specify the rivulet volumetric flow rate, Q, and either its initial contact angle, β_0, or half width, a_0.*
2. *Solve the equation* (8) *and obtain the missing variable, a_0 or β_0.*
3. *Numerically solve the differential equation* (15) *and get a set of points,*

$$\mathcal{S} = (s_i, a_i, \beta_i), \quad i = 1, 2, \ldots, N$$

Note: *In each step of the numerical solution of* (15)*, it is necessary to solve the equation* (8) *to obtain the current dynamic contact angle, β_i.*

4. *For i from 1 to N, substitute the obtained local rivulet half width, a_i, and contact angle, β_i, into the equation* (6) *and get the local gas-liquid interface shape, $\tilde{h}_i(\tilde{y})$.*

5. *In an analogy to the Algorithm 1, reconstruct the approximate gas-liquid interface position using the assumption*

$$\tilde{h}(s, \tilde{y}) \doteq \tilde{h}(s_i, \tilde{y}), \quad \forall s \in (s_i - \frac{1}{2}\delta_i, s_i + \frac{1}{2}\delta_i); \quad i = 1, 2, \ldots, N$$

4 Results and Discussion

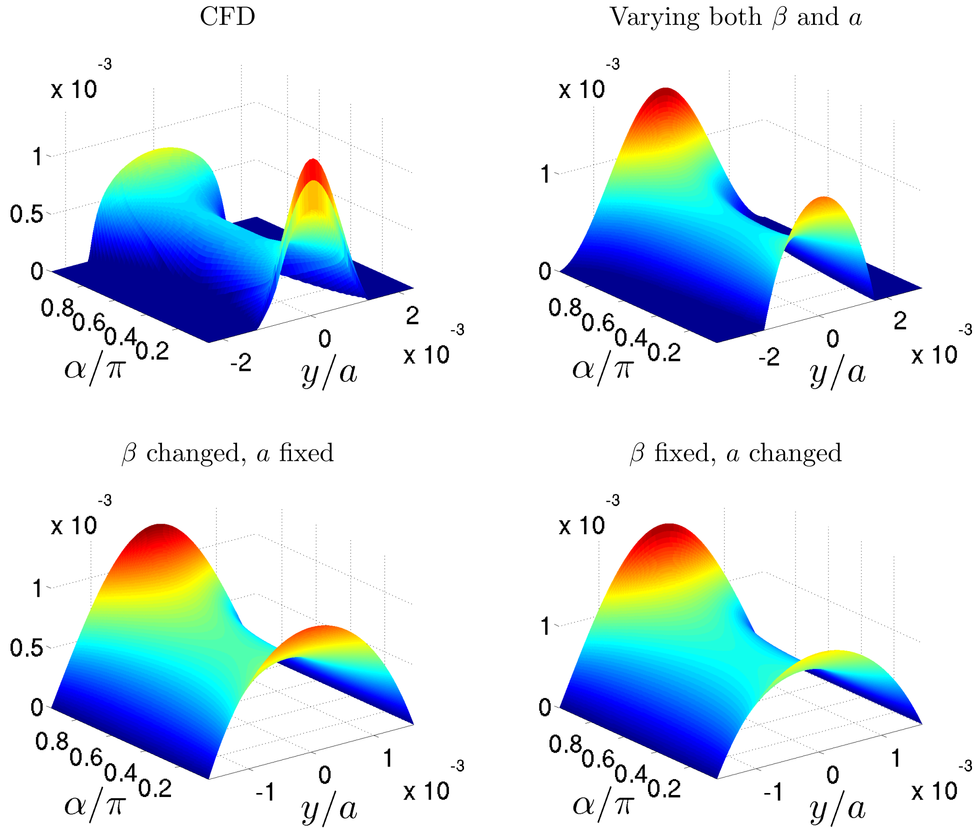

Figure 3: Comparison of rivulet free surfaces projected on a plane for all the tested methods. The case of the flow rate $Q = 1 \cdot 10^{-7}\,\mathrm{m^3 s^{-1}}$ is depicted.

A comparison of the rivulet free surface shapes for the different methods is depicted in Fig. 3. Although all the results are qualitatively the same, the methods with either a or β fixed do not seem to be as close to the CFD solution as the method with both those properties kept variable.

The problem of the model with fixed a lies mostly in the fact, that it is not able to predict the rivulet slimming with $\alpha/\pi \to 1/2_{-}$. Continuing this line of thought, the model with fixed β predicts the rivulet thinning; however, it fails to correctly estimate the magnitude of it.

Further argument favoring the model with variable both a and β can be based on the comparison of the Bond number evolution for the different methods. The agreement between the method with variable β and a and the CFD result is the best one (consult the left side of Fig. 4).

The model with constant β depicted with the dash-dotted line gives qualitatively wrong results. The graph of the dependence of B on α/π has inflection points at $\alpha/\pi \doteq 1/5$ and $\alpha/\pi \doteq 4/5$. Moreover, the predicted evolution of the rivulet Bond number is almost symmetrical around $\alpha/\pi = 1/2$. Such a symmetrical curve of dependence of B on α/π, (a) seems unphysical, as for $\alpha/\pi < 1/2$ the gravity pushes the rivulet onto the cylinder hull, and for $\alpha/\pi > 1/2$, it pulls the rivulet from the cylinder; and (b) does not correspond to the CFD result.

The model with constant a depicted with the dashed line seems to predict a qualitatively correct evolution of the rivulet Bond number. Nevertheless, it still gives a result with a symmetry around $\alpha/\pi = 1/2$ and it seems to underestimate the values of B for $\alpha/\pi > 3/4$.

As it was stated before, the results of the model with variable a and β are closest to the CFD simulation. For $\alpha/\pi < 1/2$, the $\mathrm{B} = \mathrm{B}(\alpha/\pi)$ curve predicted by the method lies almost on the top of the curve predicted by the model with fixed a and both the curves are in a good agreement with the CFD result. For $\alpha/\pi > 1/2$, the method at first overestimates the rivulet Bond number, but for $\alpha/\pi > 3/4$ the result becomes close to the CFD model again. Moreover, the $\mathrm{B} = \mathrm{B}(\alpha/\pi)$ curve predicted by the method is not symmetrical around $\alpha/\pi = 1/2$.

However, all the studied reduced models predict higher rivulet profiles maximum than CFD. This may be a result of the necessity to impose some initial liquid velocity at $\alpha = 0$ in the case of CFD.

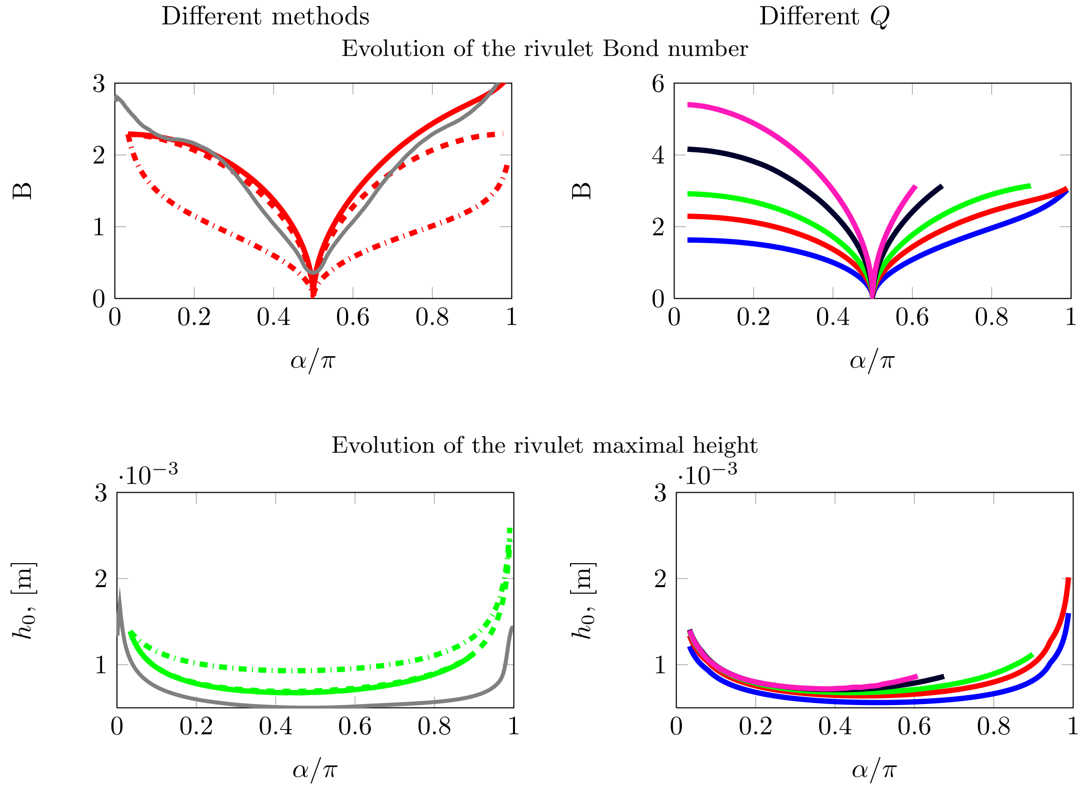

Figure 4: Evolution of the rivulet Bond number and its maximal height along the cylinder. Five different flow rates, $Q = 1 \cdot 10^{-7}$ (blue), $2 \cdot 10^{-7}$ (red), $3 \cdot 10^{-7}$ (green), $5 \cdot 10^{-7}$ (black) and $7 \cdot 10^{-7}$ (magenta) $\mathrm{m^3s^{-1}}$; and three computation methods, were compared. Solid line (——) is used for simplified calculation with both β and a varying. Results for constant a and β are denoted by (-·-·-) and (- - -), respectively. Grey lines are used to depict the corresponding CFD results.

In the right side of Fig. 4, the evolution of rivulet Bond number and the maximal profile height calculated by the model with variable both a and β is shown for various flow rates. The line ending before $\alpha/\pi = 1$ indicates liquid dripping from the cylinder.

The liquid dripping prediction by the simplified models is based on the value of the local rivulet Bond number. Let us denote the maximal profile height $\tilde{h}(s, \tilde{y} = 0) = \tilde{h}_0(s)$. From the equation (6) follows that

$$\lim_{\mathrm{B} \to \pi_-} \tilde{h}_0(s) = \infty, \quad \forall s = \alpha R \in \left(\frac{\pi R}{2}, \pi R\right). \tag{16}$$

Hence, the continuation of the solution of the surrogate models behind the point where $B = \pi$ and $\alpha/\pi > 1/2$ is not possible.

As a consequence, the simplified models can predict only the location of the initial rivulet separation point. Furthermore, as the models with fixed β or a underestimate the rivulet Bond number for $\alpha/\pi > 1/2$, their prediction of the liquid dripping is not reliable.

On the other hand, the liquid dripping in the CFD model is based on a numerical calculation of the force balance at the gas-liquid interface,

$$F_{\text{int}} = F_\gamma + F_g, \quad F_\gamma > 0, \forall s \in \left(\frac{\pi R}{2}, \pi R\right), \quad F_g < 0, \forall s \in (0, \pi)\,, \tag{17}$$

where F_{int} is the total force exerted on the gas-liquid interface, F_γ is the surface tension force and F_g is the gravity. Hence the CFD model can predict both the location of the liquid dripping and the amount of liquid which has to be removed from the film to fulfill the condition $F_\gamma - F_g > 0$.

If there are no laminar waves on the rivulet, there is a qualitative agreement beween the surrogate model with varying both β and a and the CFD simulation. At higher Q, the laminar waves cause earlier initial liquid dripping location then predicted by any of the surrogate models.

5 Conclusion

Due to the work of Duffy and Moffat [11] and Paterson et al. [12] and our previous results, we were able to derive a surrogate model for a gas-liquid interface reconstruction of a gravity-driven rivulet flowing down a monotonically varying incline without the need to fix either its width or contact angle. We compared our model to the other existing ones and to a benchmark CFD simulation. Eventhough our model is more computationally expensive than the ones already published, we believe that the additional cost is well balanced by the improvement in the model accuracy. Moreover, in our model, the solution of the complete thin film governing equation, which is a fourth order partial differential equation, was reduced to a solution of one ordinary differential equation with a solution of a non-linear algebraic equation nested in each time step. The models of Duffy and Moffat and Paterson et al. consist of a repetitive solution of a non-linear algebraic equation. Thus the difference between the computational costs of the three surrogate models is negligible compared to the cost of solving the original problem.

Nomenclature

a[m] .... half-width of the rivulet
B[$-$] .... Bond number
e[$-$] .... Euler's constant
F[N] .... force
g[m s^{-2}] .... gravitational acceleration
h[m] .... global gas-liquid interface shape function
$\tilde{h}$[m] .... local gas-liquid interface shape function
l[m] .... intermediate region length scale
n[$-$] .... normal vector
Q[m^3 s^{-1}] .... volumetric flow rate
$\hat{Q}$[$-$] .... dimensionless flow rate
s[m] .... arc length coordinate
t[s] .... time coordinate
(u, v, w)[m s^{-1}] .... velocity field
x, y, z[m] .... global coordinate system
$\tilde{x}, \tilde{y}, \tilde{z}$[m] .... local coordinate system

Greek letters

α[$-$] .... plate inclination angle
β[$-$] .... dynamic contact angle
γ[N m^{-1}] .... liquid surface tension
δ[$-$] .... small difference
κ[m^{-1}] .... surface mean curvature
λ[m] .... Navier slip length
μ[Pa s] .... liquid dynamic viscosity
ρ[kg m^{-3}] .... liquid density
τ[$-$] .... contact point for 2D interface
Ω[$-$] .... domain of rivulet solution in s direction

Acknowledgments: The presented work was supported by IGA of UCT Prague, under the grant numbers A2_FCHI_2015_026 and A1_FCHI_2015_004.

References

[1] Cooke, J. J. Gu, S. Armstrong, L. M. Luo, K. H. Gas-liqud flow on smooth and textured inclined planes, *World Ac. of Sc., Eng. and Technol.*, **2012**, *68*, 1712–1719.

[2] Maiti, R. Khanna, R. Nigam, K. P. D. Hysteresis in trickle-bed reactors: a review, *Ind. Eng. Chem. Res.*, **2006**, *45*, 5185–5198.

[3] Vlasogiannis, P. Karagiannis, G. Argyropoulos, P. Bontozoglou, V. Airwater two-phase flow and heat transfer in a plate heat exchanger, *Int. J. Multiph. Flow*, **2002**, *25*, 757–772.

[4] Kistler, S. F. Schweizer, P. M. (Eds.); *Liquid Film Coating*, Chapman and Hall, London, (1997).

[5] Ataki, A. Kolb, P. Bühlman, U. Bart, H. J. Wetting performance and pressure drop of structured packing: CFD and experiment, *I. Chem. E. – symposium series*, **2006**, *152*, 534–543.

[6] Towell, G. D. Rothfeld, L. B. Hydrodynamics of rivulet flow, *AIChE J.*, **1966**, *9*, 972–980.

[7] Allen, R. F. Biggin, C. M. Longitudinal flow of a lenticular liquid filament down an inclined plane, *Phys. Fluids*, **1974**, *17*, 287–291.

[8] Bentwich, M. Glasser, D. Kern, J. Williams, D. Analysis of Rectilinear Rivulet Flow, *Al. Che. J.* **1976**, *22* (4), 772–779.

[9] Fedotkin, I. M. Melnichuk, G. A. Koval, F. F. Klimkin E. V. Hydrodynamics of rivulet flow on a vertical surface, *Inzhenerno-Fizicheskli Zhurnal*, **1984**, *1*, 14–20.

[10] Benilov, E. S. On The Stability of Shallow Rivulets. *J. Fluid Mech.* **2009**, *636*, 455–474.

[11] Duffy, B. R. Moffat, H. K. Flow of a viscous trickle on a slowly varying incline, *Chem. Eng. J.*, **1995**, *60*, 141–146.

[12] Paterson, C. Wilson, S. K. Duffy, B. R. Pinning, de-pinning and re-pinning of a slowly varying rivulet, *Eur. J. Mech. B/Fluids*, **2013**, *41*, 94–108

[13] S.H. Davis, *Moving contact lines and rivulet instabilities, Part 1. The static rivulet*, J. Fluid Mech., Vol.90. (1980), pp.225-242.

[14] S. A. Shetty, R. L. Cerro *Spreading of liquid point sources over inclined solid surfaces* Ind. Eng. Chem. Res., Vol.34. (1995), pp. 4078-4086.

[15] M. Renardy, Y. Renardy, J. Li, *Numerical simulation of moving contact line problems using a volume-of-fluid method*, J. Comp. Phys., Vol.171. (2001), pp.243-263.

[16] K. V. Meredith, A. Heather, J. De Vries, Y. Xin, *A numerical model for partially-wetted flow of thin liquid films*, Comp. Meth. Multiph. Flow, Vol.70. (2011), pp.239-250.

[17] J. A. Diez, A. G. Gonzles, L. Kondic, *On the breakup of fluid rivulets*, Phys. Fluids, Vol.21. (2009), pp.1-15.

[18] Isoz, M.: Spreading rivulet with decrease in flow rate induced by dissipation in underlying wetting film, Proceedings of conference *TPFM 2015*, Simurda, D. Bodnar, T., Eds., Prague (2015), 77–80.

[19] Isoz, M.: Using VOF opensource code for rivulet type flow modeling., Proceedings of conference *SNA 2015*, Blaheta, R. Stary, J. Sysalova, D., Eds., Ostrava (2015), 45–48.

[20] Bonn, D. Eggers, J. Indekeu, J. Meunier, J. Rolley, E. Wetting and spreading. *Rev. Mod. Phys.*, **2009**, *81*, 739–805.

[21] Panton, R. L. Lubrication approximation. In *Incompressible Flow*, 4th ed.; John Wiley & Sons, Inc.: Hoboken, NJ, USA, 2013; pp 650–668.

[22] Huh, C. Scriven, L. E. Hydrodynamic model of steady movement of a solid/liquid/fluid contact line. *J. Col. Int. Sci.*, **1971**, *35* (11), 85–101.

[23] Voinov, O. V. Hydrodynamics of wetting. *Fluid Dyn.*, **1971**, *11*, 714–721 (English translation).

[24] Cox, R. G. The dynamics of spreading of liquids on a solid surface. Part 1. Viscous flow. *J. Fluid Mech.*, **1986**, *168*, 169–194.